

## Water quality monitoring using remote sensing, Lower Manyame Sub-catchment, Zimbabwe

H. Muhoyi <sup>a,b,\*</sup>, W. Gumindoga <sup>b</sup>, A. Mhizha <sup>b</sup>, S. N. Misi <sup>b</sup> and N. Nondo <sup>c</sup>

<sup>a</sup> Dept. of Geography and Geo-Information Sciences, Lupane State University, P.O. Box 170, Lupane, Zimbabwe

<sup>b</sup> Department of Civil Engineering, University of Zimbabwe, MP167 Mount Pleasant, Harare, Zimbabwe

<sup>c</sup> Environmental Management Agency (Zimbabwe), P.O. Box 385, Causeway, Harare, Zimbabwe

\*Corresponding author. E-mail: hmuhoiyi@gmail.com

 HM, 0000-0003-4569-1901; WG, 0000-0001-8530-7383; AM, 0000-0002-6890-5143; SNM, 0000-0002-7199-4132; NN, 0000-0002-8605-352X

### ABSTRACT

The Lower Manyame Sub-catchment (LMS) is one of the most heavily polluted in Zimbabwe. Its waters are valuable for irrigation, domestic and industrial purposes. LMS has serious eutrophication problems emanating from human activities within it, and lakes Manyame and Chivero upstream. Data collected from October 2018 to April 2019 were used to test an integrated methodology based on field measurements and remote sensing. This study illustrates the production of multitemporal spatialised maps of total suspended solids (TSS), chemical oxygen demand (COD), total nitrogen (TN) and total phosphorus (TP) concentrations from satellite data acquired from Sentinel-2. The analysis confirmed the pollution (eutrophic and organic matter) status of LMS water, for the period considered by this research. As a result, careful land planning must be done through the joint operation of local authorities, regional agencies and regional institutions, since Manyame River is a tributary of the Zambezi River (a transboundary river).

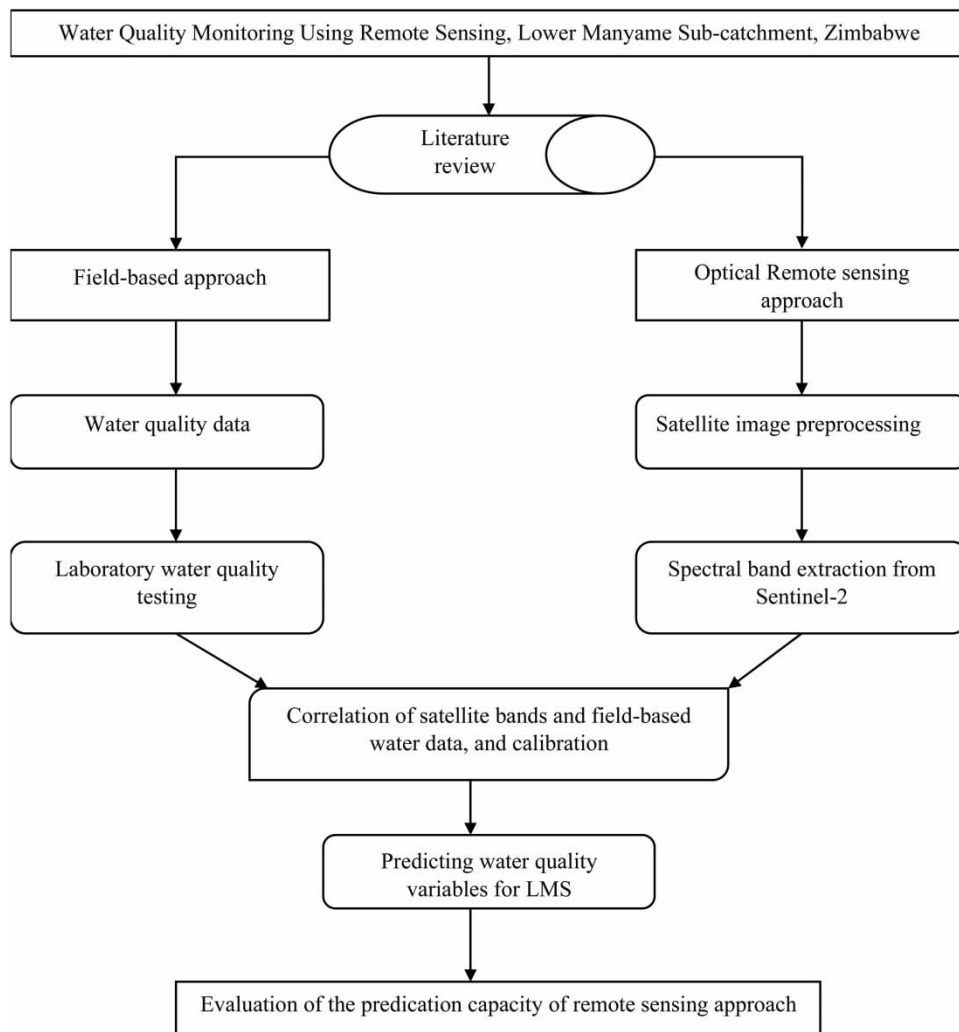
**Key words:** empirical algorithms, Lower Manyame Sub-catchment, Sentinel-2, water quality

### HIGHLIGHTS

- Lower Manyame Sub-catchment rivers are vulnerable to nutrient loading.
- This research established high phosphorous loading in the sub-catchment.
- Field data and Sentinel-2 data analysis confirmed pollution levels in LMS.
- High-resolution satellite data can be used to monitor surface water quality.

This is an Open Access article distributed under the terms of the Creative Commons Attribution Licence (CC BY-NC-ND 4.0), which permits copying and redistribution for non-commercial purposes with no derivatives, provided the original work is properly cited (<http://creativecommons.org/licenses/by-nc-nd/4.0/>).

## GRAPHICAL ABSTRACT



## INTRODUCTION

Large-scale water quality cannot be estimated correctly without suitable data acquisition. On the other hand, the application of field-based approaches, based only on frequent and/or long-term samples, cannot fully address the spatio-temporal variation of water quality in a given watershed/catchment. As a result, water monitoring, conservation and reclamation programmes need an integrated approach where long-term field-based data can be used in conjunction with cutting-edge technologies (Azanga *et al.* 2016; Sharma *et al.* 2018). It is important to collect water quality data and information when formulating and implementing pollution rehabilitation (Barrett & Frazier 2016; Meyer *et al.* 2019). Water quality monitoring is, therefore, mainly aimed at providing regular feedback to guarantee compliance with national and international water quality standards, and efficiency and effectiveness in law enforcement by different natural resources custodians.

Integrating traditional data collection with remote sensing techniques produces an efficient approach for monitoring (Azab 2012; Alikas & Kratzer 2017; Bugnot *et al.* 2018). However, traditional approaches are characterised by tiring and time-consuming fieldwork activities, thus not enabling an exhaustive description of the water bodies' quality. In addition, field-based data quality can depend on both sampling procedures and laboratory protocols (Gürsoy & Atun 2019). Sources of uncertainty include, for example, geo-location and transcription mistakes in field notes. Data acquisition by remote sensing and geographical information systems (empirical algorithms) is now common to enable rapid detection of fast changes and trends in water quality indicators in a catchment (Ortiz-Casas & Peña-Martinez 1989; Cox *et al.* 1998; Mushtaq & Nee Lala 2017). Remote-sensing-based empirical algorithms must be calibrated accurately in relation to the study area, while remote

sensing data are also weather dependent (Gholizadeh & Melesse 2017). Remote sensing has been used to assess water quality parameters in several lakes and reservoirs, nonetheless, as it can provide spatial and multitemporal information about the topmost layers of water bodies very cost-effectively. As remote sensing data are freely available, integrated approaches based on traditional field-based data collection and remote sensing are now commonly seen as suitable for water resource monitoring programs.

Sentinel-2 is a high-resolution, optical, land-mission, twin-satellite system providing 12-bit imagery in 13 spectral bands, ranging from 443 to 2,190 nm (Bande & Adam 2018). Sentinel-2A has operated since 2015 and 2B since 2017, viewing the earth's entire surface every one to two days. Data are acquired at three spatial resolutions (10, 20 and 60 m), within a viewing width of 290 km. The 10 m resolution dataset has not been used widely in studies assessing the quality in water bodies or land use land cover changes. While other satellite images – e.g., from Landsat, MERIS, MODIS, etc – have been used widely in assessing and monitoring the environment and water quality (Campbell *et al.* 2011; Andrzej *et al.* 2016; El-Zeiny & El-Kafrawy 2017; Mushtaq & Nee Lala 2017; Feng *et al.* 2019), such use of Sentinel-2 data is still in its infancy.

Correlations of satellite reflectance bands with field-based sample data have been in use for years (Meer 2001; Gholizadeh *et al.* 2016a; Deng 2019). Not all water quality parameters interact directly with the electromagnetic spectrum and yet they must be monitored. Unlike total suspended solids (TSS), chlorophyll-a/cyanobacteria and temperature, monitoring of parameters such as total nitrogen (TN), total phosphorus (TP) and biochemical oxygen demand (BOD) was challenging until correlational approaches were developed. This arises because, on the whole, only physical, rather than chemical, parameters interact directly with the electromagnetic spectrum. Many attempts have been made to establish correlations between field-based water quality data and remote-sensing reflectance band ratios (Gao *et al.* 2015; Gholizadeh *et al.* 2016b; Carstens & Amer 2019). The correlations vary from single bands, to band ratios, to complex linear regression models, and rigorous literature reviews are needed to find those algorithms that might suit an area of interest, so that the models can be calibrated and validated accordingly. Model selection must be based on model performance, as assessed by a research-based criterion. Among the criteria that can be employed are consideration of the mean root error (MRE) or coefficient of determination ( $R^2$ ), and choosing an algorithm developed in a region similar to that of interest (Azab 2012; Altansukh 2016).

Experience of using the integrated approach for water quality monitoring in the Lower Manyame Sub-catchment (LMS) is presented in this study. LMS is a vulnerable sub-catchment just above the confluence of the Manyame and Zambezi rivers. LMS is used for ecosystem sustenance, as well as irrigation, industrial, recreation and domestic purposes, so water quality monitoring has strategic importance that goes beyond ecosystem preservation. To control water quality in the country and, specifically, in LMS, the Environmental Management Agency (EMA) has and continues to use traditional field-based methods; the use of remote-sensing technology is in its infancy in most government and parastatal institutions. Therefore, the applicability of using Sentinel-2 data to estimate water quality concentrations, and integrate in-situ observations with remote-sensing data to describe water quality status were investigated this study. The empirical model results were evaluated against in-situ data collected during Sentinel-2 satellite overpasses.

## MATERIALS AND METHODS

### Study area

LMS is at the mouth of the Manyame River, at its confluence with the Zambezi River. It covers approximately 6,308 km<sup>2</sup>, and is between 29.90 and 31.20° E, and 17.00 and 16.15° S. It has both semi-arid and savannah ecosystem characteristics, with the Zambezi escarpment almost separating them. Upstream (north) of the escarpment is the near-savannah ecosystem, while the area downstream is characterised mainly by semi-arid conditions. As a result, different land uses are found in the LMS (Figure 1) where they drain into the river. The Manyame River is the main river in the LMS but the Dande River is also present. LMS has an annual mean temperature of 25 °C and 650 mm rainfall, coupled with a good soil profile, giving it high agricultural potential (Chimweta *et al.* 2018).

In Figure 1, the types of land are described using these abbreviations: AP = A1 Prime; HVPC = Highveld Prime Communal; MIM = Mutorashanga Informal Mining; NP = National Park; NZVC = Northern Zambezi Valley Communal and U = Urban. Less intense use is made of fertilisers on HVPC, NP and NZVC, except for illegal riverbank cultivation and land degradation means. AP, MIM and U offer intense pollution risk to LMS as they

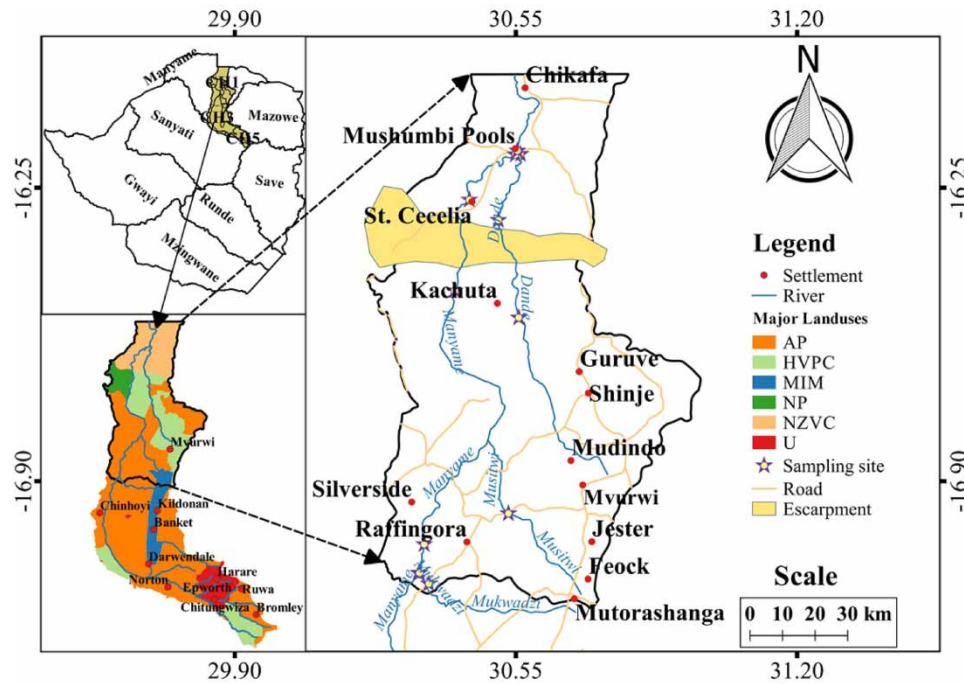


**Figure 1** | Study area, showing sampling sites and major types of land use.

are associated with high fertiliser use (AP), metal and sediment pollution (MIM) and municipal pollution from urban centres (U).

### Field data

Field data came from samples collected at 12 sites along the rivers Manyame, Dande, Musitwi and Mukwadzi (Figure 2). Standard sampling and preservations approaches were used (Kulshreshtha & Shanmugam 2018; Meyer *et al.* 2019), and the parameters – TSS, COD, TN and TP – were determined in the laboratory at the University of Zimbabwe, Department of Civil Engineering Water.

### Satellite images

The full resolution Sentinel-2 images acquired from the Earth explorer satellite image data repository for the periods October to December 2018 and January to April 2019 (Table 1), were used to define LMS river water quality. Sentinel-2 operates in the visible and near-infrared spectral range (443 to 2,190 nm), with a wavelength configuration sensitive to the most important optically active water constituents. In the subsequent literature review, existing remote sensing algorithms were evaluated and that yielding the highest value of  $R^2$  selected for use. Only cloud-free images that coincided with field-based data collection dates were used (Bonansea *et al.* 2019).

Following other studies (Ortiz-Casas & Peña-Martinez 1989; Banko 1998; Gao *et al.* 2015; Feng *et al.* 2019), image pre-processing routines were carried out using the Quantum Geographical Information System (QGIS). The QGIS semi-automatic plugin was used to convert the radiance Sentinel-2 satellite imagery data to Earth's surface reflectance – i.e., correcting irradiance to all bands – which accounts for the difference between the actual and nominal solar irradiance wavelengths in each channel, and the top of atmosphere reflectance. The pre-processed images were analysed using existing empirical algorithms (Table 2) to estimate the concentrations of TSS, COD, TN and TP.

## RESULTS AND DISCUSSION

### Analysis and validation

#### TSS

Findings from both the field and remote sensing showed that TSS concentrations were very low (Figure 3), the range observed was from 0.59 to 1.42 mg/L. TSS varied differently across the catchment, with relatively high

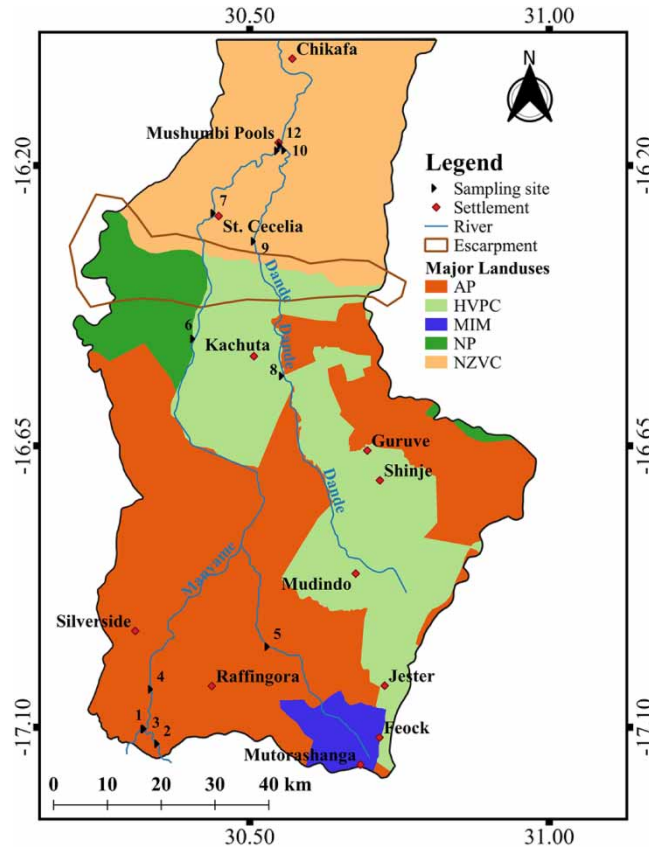


Figure 2 | LMS sampling sites.

Table 1 | Field sampling dates in line with Sentinel-2 revisit calendar

2018	18-Oct	05-Dec	18-Dec
2019	27-Jan	13-Feb	18-April

Table 2 | The modified empirical algorithms used

Adjusted algorithms	Source	R-squared
$TSS = 4.83 - 10.09*B3 - 0.37*B4 - 3.32*(B2/B3)$	Song <i>et al.</i> (2014)	0.27
$COD = 218.75 - 4271.43*B2 + 3214.16*B3 - 561.44*B4$	Wang <i>et al.</i> (2004)	0.21
$TN = \exp(1.10*(B4/B2) - 0.30*(B2/B4) - 3.16*B4 - 0.40)$	Torbick <i>et al.</i> (2013)	0.47
$TP = \exp(2.53 + 1.94*B4 - 0.97*(B4/B2) - 1.42*(B2/B4))$	Torbick <i>et al.</i> (2013)	0.55

concentrations observed in zones adjacent to areas that were recently deforested, semi-arid and/or close to mining activities. TSS concentrations were also higher in the Dande than the Manyame River, possibly as a result of river catchment characteristics such as sparser vegetation and mining activities (Zwane *et al.* 2006); so that areas drained by the Dande River yield high sediment loads since they are in the semi-arid region.

**COD**

Figure 4 shows some detailed COD results in the study area. The concentration range observed was from 37 to 142 mg/L. The high COD concentrations in the Dande River should be considered with caution as the river is dry most of the time, so there may be inconsistencies in COD determination using remote sensing. However, it can also be argued that Dande River water had high COD concentrations because only a few perennial streams feed

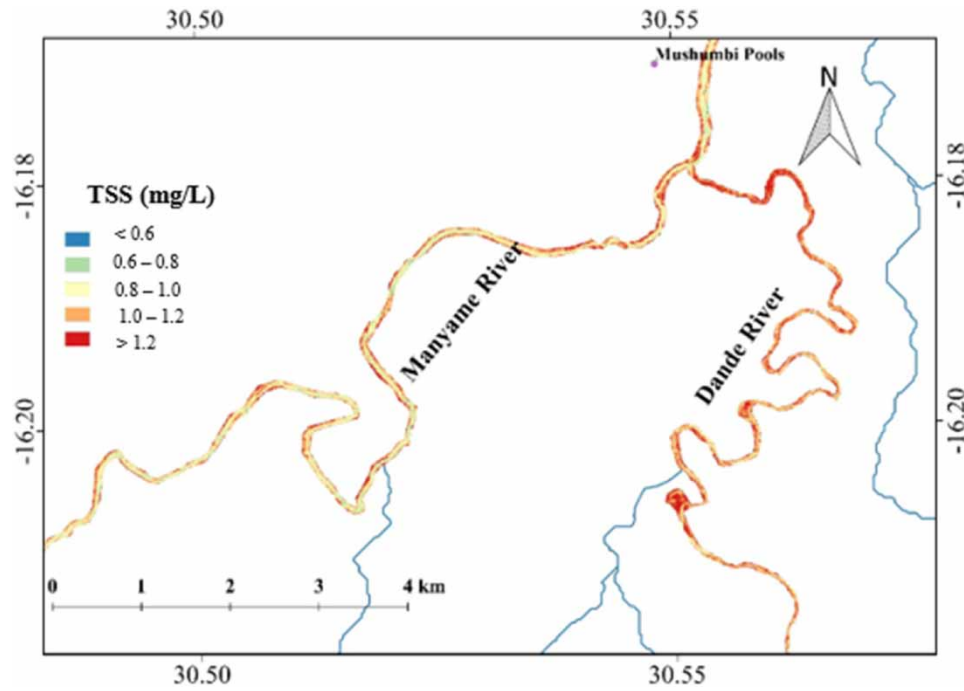


**Figure 3** | TSS (mg/L).

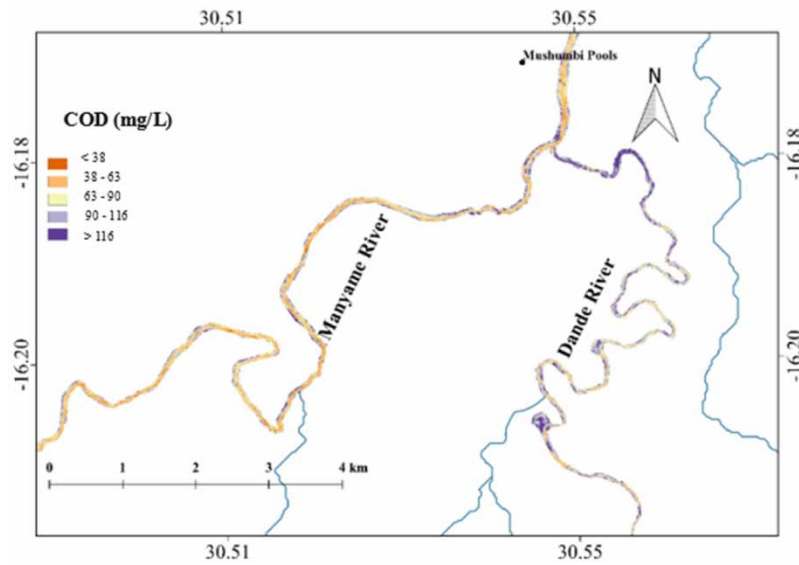


**Figure 4** | COD (mg/L).

it. Pollutants in the Dande are relatively concentrated, unlike the Manyame River, which is fed by streams such as the Musitwi and Mukwadzi upstream of the Dande River confluence.

#### TN

Figure 5 shows TN concentrations in part of LMS where concentrations ranged from 0.42 to 1.06 mg/L. TN concentrations are relatively lower in the Manyame River than in the Dande River. As for COD, this can be attributed to the Dande's low discharge and lack of effective contributing streams. The TN concentrations observed in the LMS water could arise from anthropogenic activities including fertiliser use, animal husbandry and industrial effluents.

#### TP

TP concentrations ranged from 1.00 to 3.45 mg/L (Figure 6), suggesting that river water in LMS is eutrophic. This could result from the extensive agricultural activities there, with some irrigated zones, and also, possibly,

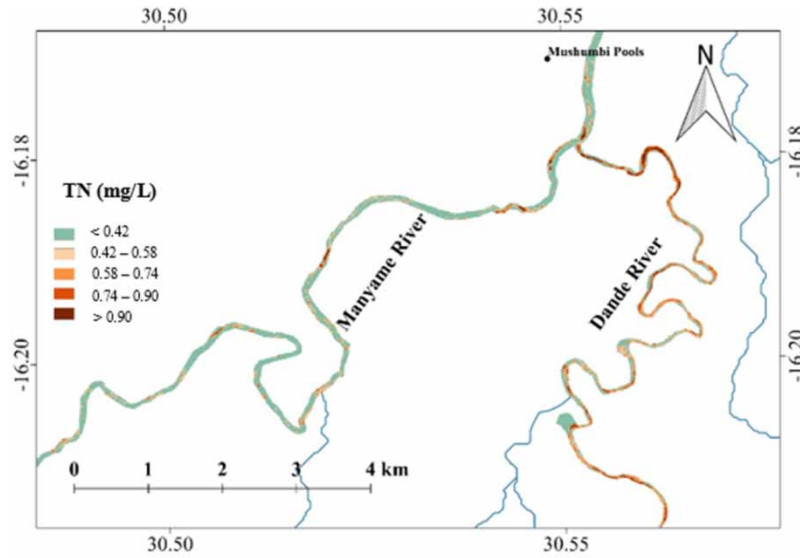


**Figure 5** | TN (mg/L).

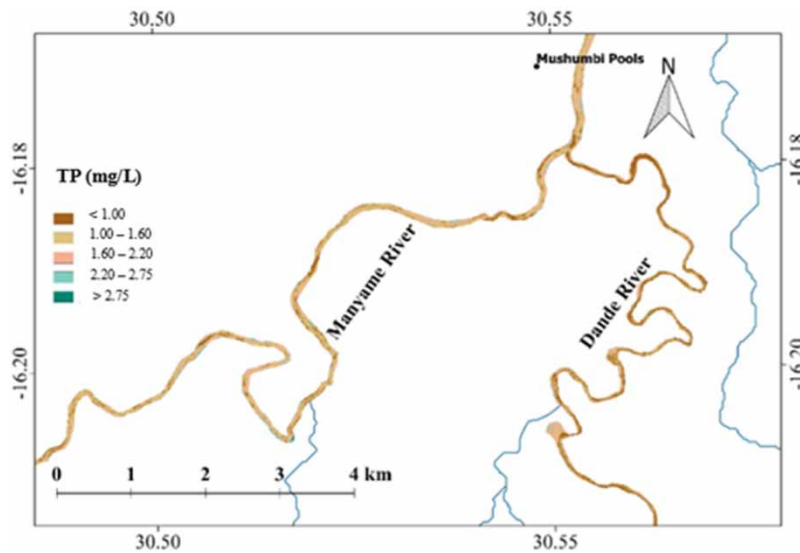


**Figure 6** | TP (mg/L).

sediment transport with nutrient particulates attached (Song *et al.* 2012; Ak 2017; Cui *et al.* 2018). Agricultural sources of TP contribute immediately to eutrophication as the nutrients, which are dissolved, are readily available to aquatic vegetative organisms (Ebrahimi *et al.* 2022). On the other hand, TP from weathering and other particulate matter, as found in sediment transport, are affected by the underlying environmental conditions as they first need to decompose before the nutrient is readily available for use – i.e., in soluble form (Lee & Oh 2018).

### Relationships between remote-sensing and field-based water quality parameters

The water quality parameter values predicted from remote sensing (Sentinel-2) correlated well with the field-based results.  $R^2$  ranged from 0.63 for TP to 0.78 for TN (Figure 7). The correlations indicated that the remote-sensing results tended to underestimate the highest water quality parameter concentrations while generalising the lowest ones. However, this could result in part from the field data's high variability, which may be influenced by the distances and different human activities between the sampling points. This was explained well by the high SDs of field-based parameter results (Table 3). Giardino *et al.* (2012) also found that field-based analyses may be inaccurate. Therefore, this study confirms that the high multi-spectral resolution Sentinel-2 information can be used to predict water quality parameters in LMS.

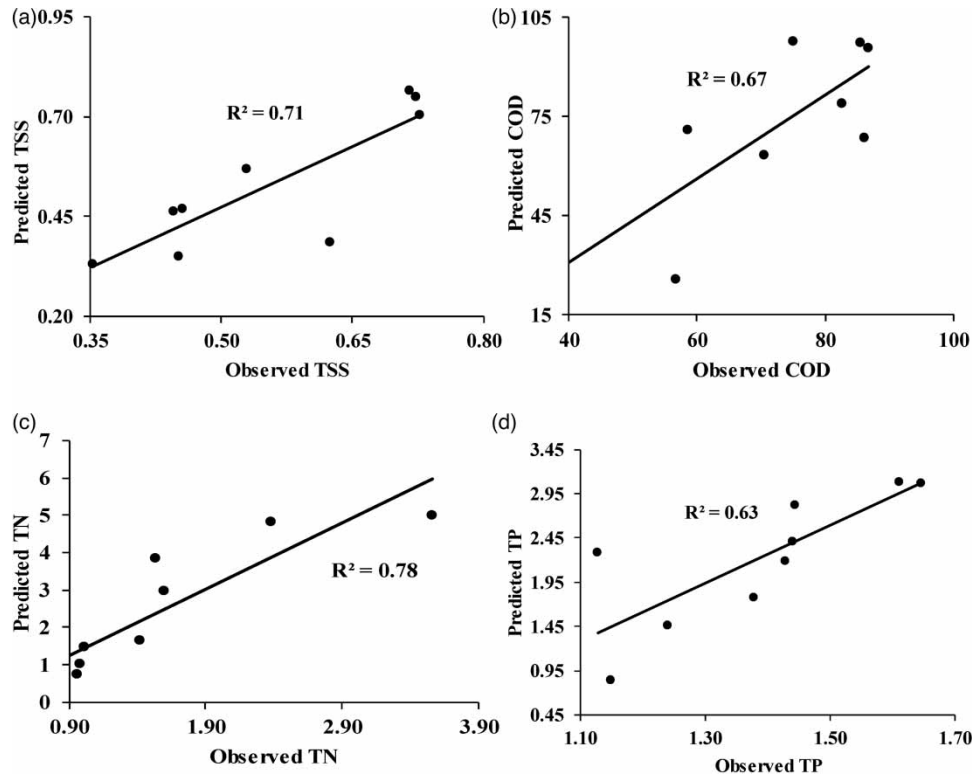


**Figure 7** | Comparison between the measured and remote-sensing derived water quality concentrations, where (a) = TSS, (b) = COD, (c) = TN, and (d) = TP.

**Table 3** | Site-based water quality variable concentrations from field-sampling and Sentinel-2 images

Station ID	In-situ	Sentinel-2	Parameter
6	0.27 ± 0.02	0.37 ± 0.17	TSS
7	0.27 ± 0.02	0.16 ± 0.17	
8	0.31 ± 0.02	0.50 ± 0.17	
6	12.00 ± 26.18	24.73 ± 26.44	COD
7	13.35 ± 26.18	30.36 ± 26.44	
8	58.00 ± 26.18	73.07 ± 26.44	
6	5.40 ± 2.45	3.45 ± 0.14	TN
7	1.23 ± 2.45	3.41 ± 0.14	
8	1.10 ± 2.45	3.19 ± 0.14	
6	0.05 ± 1.99	2.17 ± 0.04	TP
7	4.02 ± 1.99	2.10 ± 0.04	
8	1.92 ± 1.99	2.11 ± 0.04	

**Validation**

Three of the nine sites were purposively selected to validate the results. Sites 6 (Manyame River) and 8 (Dande River) were selected to represent water quality from remote sensing upstream of the escarpment. Site 7 (Manyame River) was selected as being close to a confluence of the numerous minor tributaries feeding the Manyame River. Site 7 is also downstream of the escarpment and there was a need to assess whether remote sensing approaches can quantify water quality pollution as effected by both the escarpment and the contributions of the tributaries.

The results of applying the empirical algorithms to the satellite images, corrected previously for atmospheric effects, were compared to the related field-based results. Table 3 shows the field-based TSS, COD, TN and TP



values vs those predicted by Sentinel-2, and their respective SDs, for stations 6, 7 and 8 on LMS surface water (Figure 2). The largest deviations were observed for the field-based sampling values, probably due to large distances between sampling points, which resulted in different pollution levels as impacted by local human activities, among other factors.

### Remote sensing and surface water monitoring for LMS

Water quality in rivers generally varies significantly over time at individual sites or along reaches, as induced by but not limited to streamflow, pollution source availability and/or hydrologic process in the catchment (Bugnot *et al.* 2018; Liu *et al.* 2018). Spatio-temporal variation in surface water quality is relevant when site-specific management strategies are to be developed. Although several different satellite image sets can be used for surface water quality assessment, those from Sentinel-2 are gaining wide use as they have high spatio-temporal resolution compared to others – e.g., Landsat. Sentinel-2's five-day temporal resolution is important in surface water quality monitoring, especially for rivers passing through areas with different anthropogenic activities and transboundary rivers like the Manyame River. Theoretically, the Manyame River is heavily polluted from Harare (upstream) to Mushumbi Pools (downstream). In this study, however, the spatio-temporal variation analysis showed that its tributaries were more heavily polluted than the Manyame itself. This could arise partly because most of the Manyame's tributaries are dry most of the year. As a result, the reflectance captured in the satellite images may be that of the dry river bed rather than water, resulting in compromised water quality information.

Most remote-sensing approaches can be used with different satellite images. While Landsat TM dominated this domain previously because of its low cost, and temporal and spatial resolutions, Sentinel-2 can do much better. In fact, remote-sensing spatio-temporal analysis can yield acceptable results for perennial rivers of varied width and depth (Beck 1987; Shafique *et al.* 2002; Gholizadeh *et al.* 2016a; Sharma *et al.* 2018). In this study, high spatial resolution satellite images were used to capture spatial variation in pollution parameters along the main rivers of LMS.

### CONCLUSIONS

This study confirmed the effectiveness of an integrated approach based on remote sensing and *in situ* measurements to evaluate water quality in LMS. The integrated approach allows natural resource custodians to take advantage of the use of multi-temporal, remote-sensing data – a cost-effective technology that has been shown to be an important source of information to support the definition of water quality status in LMS.

It has been shown that tributaries can hold the balance of power, acting as vectors from different pollution sources, whether point-based or diffuse, or organic or inorganic.

### ACKNOWLEDGEMENTS

Gratitude goes to the Environmental Management Agency and DUPC (through the S-MultiStor Project) for the assistance rendered in this study, especially the funding.

### FUNDING

Support for this research (data collection) was received from Environmental Management Agency and DUPC (S-MultiStor Project).

### CONFLICT OF INTEREST STATEMENT

The authors declare there is no conflict.

### DATA AVAILABILITY STATEMENT

Data cannot be made publicly available; readers should contact the corresponding author for details.

### REFERENCES

- Ak, R. 2017 Evaluation of TSS, BOD5, and TP in sewage effluent receiving Sambul River. *J. Pollut. Eff. Control* **05**, 1–5. <https://doi.org/10.4172/2375-4397.1000189>.
- Alikas, K. & Kratzer, S. 2017 Improved retrieval of Secchi depth for optically-complex waters using remote sensing data. *Ecol. Indic.* **77**, 218–227. <https://doi.org/10.1016/j.ecolind.2017.02.007>.

- Altansukh, O. 2016 Surface water quality assessment and modelling A case study in the Tuul River, Ulaanbaatar city, Mongolia. *Philos. Sci.* **81**, 105.
- Andrzej, U. J., Wochna, A., Bubak, I., Grzybowski, W., Lukawska-Matuszewska, K., Łacka, M., Śliwińska, S., Wojtasiewicz, B. & Zajaczkowski, M. 2016 Application of landsat 8 imagery to regional-scale assessment of lake water quality. *Int. J. Appl. Earth Obs. Geoinformation* **51**, 28–36. <https://doi.org/10.1016/j.jag.2016.04.004>.
- Azab, A. 2012 *Integrating GIS, Remote Sensing, and Mathematical Modelling for Surface Water Quality Management in Irrigated Watersheds (PhD)*. Delft, Netherlands. <https://doi.org/10.1201/b11797>
- Azanga, E., Majaliwa, M., Kansime, F., Mushagalusa, N., Karume, K. & Tenywa, M. M. 2016 Land-use and land cover, sediment and nutrient hotspot areas changes in Lake Tanganyika Basin. *Afr. J. Rural Dev.* **1**, 75–90.
- Bande, P. & Adam, E. 2018 Comparing Landsat 8 and sentinel-2 in mapping water quality at Vaal Dam. *IEEE* **7**, 9280–9285.
- Banko, G. 1998 A review of assessing the accuracy of classifications of remotely sensed data and of methods including remote sensing data in forest inventory. *New Sci.* **89**, 26.
- Barrett, D. & Frazier, A. 2016 Automated method for monitoring water quality using landsat imagery. *Water* **8**, 257. <https://doi.org/10.3390/w8060257>.
- Beck, M. B. 1987 Water quality modeling: a review of the analysis of uncertainty. *Water Resour. Res.* **23**, 1393–1442.
- Bonanse, M., Ledesma, M., Rodriguez, C. & Pinotti, L. 2019 Using new remote sensing satellites for assessing water quality in a reservoir. *Hydrol. Sci. J.* **64**, 34–44. <https://doi.org/10.1080/02626667.2018.1552001>.
- Bugnot, A. B., Lyons, M. B., Scanes, P., Clark, G. F., Fyfe, S. K., Lewis, A. & Johnston, E. L. 2018 A novel framework for the use of remote sensing for monitoring catchments at continental scales. *J. Environ. Manage.* **217**, 939–950. <https://doi.org/10.1016/j.jenvman.2018.03.058>.
- Campbell, G., Phinn, S. R., Dekker, A. G. & Brando, V. E. 2011 Remote sensing of water quality in an Australian tropical freshwater impoundment using matrix inversion and MERIS images. *Remote Sens. Environ.* **115**, 2402–2414. <https://doi.org/10.1016/j.rse.2011.05.003>.
- Carstens, D. & Amer, R. 2019 Spatio-temporal analysis of urban changes and surface water quality. *J. Hydrol.* **569**, 720–734. <https://doi.org/10.1016/j.jhydrol.2018.12.033>.
- Chimweta, M., Nyakudya, I. W. & Jimu, L. 2018 Fertility status of cultivated floodplain soils in the Zambezi Valley, northern Zimbabwe. *Phys. Chem. Earth Parts ABC* **105**, 147–153. <https://doi.org/10.1016/j.pce.2017.12.005>.
- Cox, R. M., Forsythe, R. D., Vaughan, G. E. & Olmsted, L. L. 1998 Assessing water quality in catabwa river reservoirs using landsat thematic mapper satellite data. *Lake Reserv. Manag.* **14**, 405–416. <https://doi.org/10.1080/07438149809354347>.
- Cui, G., Wang, X., Li, C., Li, Y., Yan, S. & Yang, Z. 2018 Water use efficiency and TN/TP concentrations as indicators for watershed land-use management: a case study in Miyun District, north China. *Ecol. Indic., Multi-Scale Ecological Indicators for Supporting Sustainable Watershed Management* **92**, 239–253. <https://doi.org/10.1016/j.ecolind.2017.05.006>.
- Deng, X. 2019 Correlations between water quality and the structure and connectivity of the river network in the Southern Jiangsu Plain, Eastern China. *Sci. Total Environ.* **664**, 583–594. <https://doi.org/10.1016/j.scitotenv.2019.02.048>.
- Ebrahimi, E., Asadi, H., Joudi, M., Rashti, M. R., Farhangi, M. B., Ashrafzadeh, A. & Khodadadi, M. 2022 Variation entry of sediment, organic matter and different forms of phosphorus and nitrogen in flood and normal events in the Anzali wetland. *J. Water Clim. Change* **13**, 434–450. <https://doi.org/10.2166/wcc.2021.456>.
- El-Zeiny, A. & El-Kafrawy, S. 2017 Assessment of water pollution induced by human activities in Burullus Lake using Landsat 8 operational land imager and GIS. *Egypt. J. Remote Sens. Space Sci.* **20**, 49–56. <https://doi.org/10.1016/j.ejrs.2016.10.002>.
- Feng, L., Hou, X. & Zheng, Y. 2019 Monitoring and understanding the water transparency changes of fifty large lakes on the Yangtze Plain based on long-term MODIS observations. *Remote Sens. Environ.* **221**, 675–686. <https://doi.org/10.1016/j.rse.2018.12.007>.
- Gao, Y., Gao, J., Yin, H., Liu, C., Xia, T., Wang, J. & Huang, Q. 2015 Remote sensing estimation of the total phosphorus concentration in a large lake using band combinations and regional multivariate statistical modeling techniques. *J. Environ. Manage.* **151**, 33–43. <https://doi.org/10.1016/j.jenvman.2014.11.036>.
- Gholizadeh, M. H. & Melesse, A. M. 2017 Study on spatiotemporal variability of water quality parameters in florida bay using remote sensing. *J. Remote Sens. GIS* **06**, 1–12. <https://doi.org/10.4172/2469-4134.1000207>.
- Gholizadeh, M., Melesse, A. & Reddi, L. 2016a A comprehensive review on water quality parameters estimation using remote sensing techniques. *Sensors* **16**, 1298. <https://doi.org/10.3390/s16081298>.
- Gholizadeh, M., Melesse, A. & Reddi, L. 2016b A comprehensive review on water quality parameters estimation using remote sensing techniques. *Sensors* **16**, 1298. <https://doi.org/10.3390/s16081298>.
- Giardino, C., Candiani, G., Bresciani, M., Lee, Z., Gagliano, S. & Pepe, M. 2012 BOMBER: A tool for estimating water quality and bottom properties from remote sensing images. *Comput. Geosci.* **45**, 313–318. <https://doi.org/10.1016/j.cageo.2011.11.022>.
- Gürsoy, Ö. & Atun, R. 2019 Investigating surface water pollution by integrated remotely sensed and field spectral measurement data: a case study. *Pol. J. Environ. Stud.* **28**, 2139–2144. <https://doi.org/10.15244/pjoes/90598>.
- Kulshreshtha, A. & Shanmugam, P. 2018 Assessment of trophic state and water quality of coastal-inland lakes based on fuzzy inference system. *J. Gt. Lakes Res.* **44**, 1010–1025. <https://doi.org/10.1016/j.jglr.2018.07.015>.
- Lee, J.-K. & Oh, J.-M. 2018 A study on the characteristics of organic matter and nutrients released from sediments into agricultural reservoirs. *Water* **10**, 980. <https://doi.org/10.3390/w10080980>.
- Liu, S., Ryu, D., Webb, J. A., Lintern, A., Waters, D., Guo, D. & Western, A. W. 2018 Characterisation of spatial variability in water quality in the Great Barrier Reef catchments using multivariate statistical analysis. *Mar. Pollut. Bull.* **137**, 137–151. <https://doi.org/10.1016/j.marpolbul.2018.10.019>.

- Meer, F. 2001 Spectral matching using pixel cross-correlograms for the analysis of LANDSAT TM data. *Int. J. Appl. Earth Obs. Geoinformation* **3**, 197–202. [https://doi.org/10.1016/S0303-2434\(01\)85012-1](https://doi.org/10.1016/S0303-2434(01)85012-1).
- Meyer, A. M., Klein, C., Fünfroeken, E., Kautenburger, R. & Beck, H. P. 2019 Real-time monitoring of water quality to identify pollution pathways in small and middle scale rivers. *Sci. Total Environ.* **651**, 2323–2333. <https://doi.org/10.1016/j.scitotenv.2018.10.069>.
- Mushtaq, F. & Nee Lala, M. G. 2017 Remote estimation of water quality parameters of Himalayan lake (Kashmir) using Landsat 8 OLI imagery. *Geocarto Int.* **32**, 274–285. <https://doi.org/10.1080/10106049.2016.1140818>.
- Ortiz-Casas, J. L. & Peña-Martinez, R. 1989 Water quality monitoring in spanish reservoirs by satellite remote sensing. *Lake Reserv. Manag.* **5**, 23–29. <https://doi.org/10.1080/07438148909354395>.
- Shafique, N. A., Fulk, F., Autrey, B. C. & Flotemersch, J. 2002 Hyperspectral remote sensing of water quality parameters for large rivers in the Ohio River Basin. *Environ. Prot. Agency USA* **4**, 216–221.
- Sharma, B., Kumar, M., Denis, D. M. & Singh, S. K. 2018 Appraisal of river water quality using open-access earth observation data set: a study of river Ganga at Allahabad (India). *Sustain. Water Resour. Manag.* **8**, 1–12. <https://doi.org/10.1007/s40899-018-0251-7>.
- Song, C., Huang, B., Ke, L. & Richards, K. S. 2014 Remote sensing of alpine lake water environment changes on the Tibetan Plateau and surroundings: a review. *ISPRS J. Photogramm. Remote Sens.* **92**, 26–37. <https://doi.org/10.1016/j.isprsjprs.2014.03.001>.
- Song, K., Li, L., Li, S., Tedesco, L., Hall, B. & Li, L. 2012 Hyperspectral remote sensing of total phosphorus (TP) in three central indiana water supply reservoirs. *Water. Air. Soil Pollut.* **223**, 1481–1502. <https://doi.org/10.1007/s11270-011-0959-6>.
- Torbick, N., Hession, S., Hagen, S., Wiangwang, N., Becker, B. & Qi, J. 2013 Mapping inland lake water quality across the lower peninsula of michigan using landsat TM imagery. *Int. J. Remote Sens.* **34**, 7607–7624. <https://doi.org/10.1080/01431161.2013.822602>.
- Wang, Y., Xia, H., Fu, J. & Sheng, G. 2004 Water quality change in reservoirs of Shenzhen, China: detection using LANDSAT/TM data. *Sci. Total Environ.* **328**, 195–206. <https://doi.org/10.1016/j.scitotenv.2004.02.020>.
- Zwane, N., Love, D., Hoko, Z. & Shoko, D. 2006 Managing the impact of gold panning activities within the context of integrated water resources management planning in the Lower Manyame Sub-Catchment, Zambezi Basin. *Zimbabwe. Phys. Chem. Earth Parts ABC* **31**, 848–856. <https://doi.org/10.1016/j.pce.2006.08.024>.

First received 21 April 2022; accepted in revised form 29 May 2022. Available online 3 June 2022